



Calcium-induced transformation of cardiolipin nanodisks

Colin A. Fox^a, Patricia Ellison^a, Nikita Ikon^b, Robert O. Ryan^{a,*}

^a Department of Biochemistry and Molecular Biology, University of Nevada, Reno, Reno, NV 89557, United States of America

^b Department of Nutritional Sciences and Toxicology, University of California, Berkeley, Berkeley, CA, United States of America

ARTICLE INFO

Keywords:

Cardiolipin
Nanodisk
Calcium
Apolipoprotein A-I
Bilayer
Hexagonal II phase

ABSTRACT

Miniature membranes comprised of tetramyristoylcardiolipin (CL) and apolipoprotein (apo) A-I, termed nanodisks (ND), are stable, aqueous soluble, reconstituted high density lipoproteins. When CL ND, but not dimyristoylphosphatidylcholine (PC) ND, were incubated with CaCl₂, a concentration dependent increase in sample turbidity occurred, consistent with CL undergoing a bilayer to non-bilayer transition. To assess the cation specificity of this reaction, CL ND were incubated with various mono- and divalent cations. Whereas monovalent cations had no discernable effect, MgCl₂ and SrCl₂ induced a response similar to CaCl₂. When ND were formulated using different weight ratios of CL and PC, those possessing 100% CL or 75% CL remained susceptible to CaCl₂ induced sample turbidity development while ND possessing 50% CL displayed reduced susceptibility. ND comprised of 25% CL and 75% PC were unaffected by CaCl₂ under these conditions. SDS PAGE analysis of insoluble material generated by incubation of CL ND with CaCl₂ revealed that nearly all apoA-I was recovered in the insoluble fraction along with CL. One h after addition of EDTA to CaCl₂-treated CL ND, sample clarity was restored. Collectively, the data are consistent with a model wherein Ca²⁺ forms a bidentate interaction with anionic phosphates in the polar head group of CL. As phosphate group repositioning occurs to maximize Ca²⁺ binding, CL acyl chains reposition, accentuating the conical shape of CL to an extent that is incompatible with the ND bilayer structure.

1. Introduction

Cardiolipin (CL) is a uniquely structured glycerophospholipid that localizes to the inner membrane of mitochondria [1]. Unlike other phospholipids, cardiolipin possesses two phosphates, three glycerols and four fatty acyl chains. Due to its relatively small polar head group and four esterified fatty acids, CL possesses a “cone-shaped” molecular structure [2,3]. As a result, CL is considered to be a “non-bilayer” phospholipid that, when present in a bilayer setting, exerts negative curvature pressure [4]. Whereas CL is not well accommodated in planar bilayer membranes [5], it is a key component of highly curved bilayers such as the cristae membranes of mitochondria [6].

Calcium plays an important role in mitochondrial signaling and function [7]. Mitochondrial calcium overload is known to induce apoptosis and it is conceivable that interactions between calcium, CL and cytochrome *c* are involved in molecular events that trigger apoptosis [8–10]. Interaction of calcium with CL containing liposomes is known to induce a bilayer to non-bilayer transition, resulting in formation of an inverted hexagonal II lipid phase [11–13]. The molecular

basis for this phenomenon is not fully understood and, to date, most studies have been performed using liposomes that possess varying percentages (typically ~20%) of their phospholipid mass as CL [14–16]. One of the limitations associated with liposomes as a model system is the fact that up to one half of the bilayer phospholipid content resides in the inner monolayer leaflet where it is largely inaccessible to the external environment. In the case of multilamellar vesicles, an even greater proportion of liposomal phospholipid is inaccessible. Additionally, liposomes often display polydispersity, exhibit limited stability and scatter light to varying degrees, indicating a lack of complete solubility [17–19].

By contrast, recent studies have shown that CL can be fully solubilized in aqueous buffer upon incorporation into nanoscale membrane complexes comprised solely of CL and apolipoprotein (apo) A-I [20]. These complexes, termed nanodisks (ND), exist as disk-shaped phospholipid bilayers whose perimeter is circumscribed by an amphipathic scaffold protein, such as apoA-I [21]. Although CL is generally unstable in a planar bilayer setting, the apolipoprotein scaffold appears to exert a stabilizing force, effectively serving as a “belt” around the perimeter of

Abbreviations: CL, tetramyristoylcardiolipin; PC, dimyristoylphosphatidylcholine; ND, nanodisk; ApoA-I, apolipoprotein A-I

* Corresponding author at: Biochemistry and Molecular Biology, University of Nevada, Reno, Mail Stop 0330, 1664 N. Virginia Street, Reno, NV 89557, United States of America.

E-mail address: robertryan@unr.edu (R.O. Ryan).

<https://doi.org/10.1016/j.bbamem.2019.03.005>

Received 1 February 2019; Received in revised form 8 March 2019; Accepted 11 March 2019

Available online 13 March 2019

0005-2736/ © 2019 Elsevier B.V. All rights reserved.

the discoidal bilayer. Compared to liposomes, CL ND have inherent advantages for studies of molecular interactions, including a uniform nanoscale particle size distribution, complete aqueous solubility, ease of formulation, the absence of an inaccessible bilayer leaflet and, most remarkably, ND can be generated using CL as the sole lipid component. In the present study, CL ND were employed as a model system to investigate the effect of CaCl_2 on CL ND structure, stability and aqueous solubility.

2. Materials and methods

2.1. Nanodisk formulation

Dimyristoylphosphatidylcholine (PC), tetramyristoyl cardiolipin (CL) and tetralinoleoyl cardiolipin were purchased from Avanti Polar Lipids. Unless otherwise indicated, studies reported herein employed tetramyristoyl CL. Five mg aliquots were dissolved in 200 μL $\text{CHCl}_3:\text{CH}_3\text{OH}$ (3:1 v/v), and dried under a stream of N_2 gas, creating a thin film on the walls of the vessel. Samples were lyophilized overnight to remove residual solvent. To formulate ND, 750 μL 20 mM HEPES buffer, pH 7.2, was added to a 5 mg aliquot of dried phospholipid. The sample was vortexed to disperse the phospholipid which ultimately appeared as an opaque suspension. Subsequently, 2 mg recombinant human apoA-I [22] in 500 μL HEPES buffer was added to the lipid suspension. The final volume of the mixture was 1.25 ml. PC ND were formulated by bath sonication of the PC/apoA-I mixture at 25 °C until the solution cleared (< 10 min). Tetramyristoyl CL ND (hereafter referred to as CL ND) were formulated in a similar manner, with the exception that bath sonication was performed at 48 °C. Tetralinoleoyl CL ND were formulated by bath sonication at 25 °C under an N_2 atmosphere.

2.2. Gel filtration chromatography of ND samples

ND samples, formulated as above, were centrifuged at 14,000 $\times g$ for 2 min prior to gel permeation chromatography on a Superose 6 Increase 10/300 GL column using a GE AKTA Pure FPLC instrument. Two hundred μL ND (corresponding to 0.8 mg CL), were applied to the column. Samples were chromatographed in 20 mM HEPES at a flow rate of 0.5 mL/min with absorbance monitored at 280 nm and collection of 1.0 mL fractions.

2.3. Incubation of ND with cations

Following formulation of ND, 25 μL aliquots (100 μg phospholipid; corresponding to 78 nmol CL or 147 nmol PC) were added to the wells of a UV Star microtiter plate (Greiner Bio-One). Indicated amounts of CaCl_2 were added to the wells. The final volume of all wells was maintained at 200 μL through addition of HEPES buffer. After addition of HEPES and CaCl_2 , samples were incubated for 1 h at 22 °C or 37 °C. Sample turbidity was measured as absorbance at 325 nm using a Spectramax M5 microplate reader. Background absorbance at 325 nm, determined in wells containing deionized water, was < 0.05. To determine the effect of other cations, ND were added to a microtiter plate as described above. The chloride salt of specified mono- or divalent cations were added to the wells, samples incubated for 1 h at 22 °C and absorbance measured at 325 nm (i.e. turbidity). To assess partitioning of the apoA-I scaffold protein following CaCl_2 -induced CL ND sample turbidity development, 25 μL CL ND (equivalent to 78 nmol CL) were incubated with 2000 nmol CaCl_2 in a final volume of 200 μL for 1 h at 22 °C. The turbid sample was centrifuged at 14,000 $\times g$ for 2 min to pellet insoluble material. The supernatant was recovered and the pellet re-suspended in 200 μL HEPES buffer. Ten μL aliquots of the supernatant and resuspended pellet were electrophoresed on a 4–20% SDS PAGE slab gel and stained with GelCode Blue Stain Reagent (Thermo). Gel images were documented on a GE Healthcare Typhoon Trio

Variable Mode Imager. To assess the relative distribution of apoA-I in CaCl_2 disrupted CL ND supernatant and pellet fractions, densitometric analysis of gel band intensity was performed using ImageJ software [23]. To measure the relative distribution of CL between pellet and supernatant fractions generated by incubation of CL ND with CaCl_2 , the CL specific fluorescent dye, 10-N-nonyl acridine orange [24] (Thermo) was employed. Samples were excited at 499 nm and emission monitored from 530 nm to 610 nm on a Spectramax M5 microplate reader in a fluorescence compatible microtiter plate (Greiner Bio-One).

2.4. Incubation of mixed phospholipid ND with CaCl_2

To assess the effect of CaCl_2 on mixed phospholipid ND, different weight ratios of CL and PC were used to formulate “mixed lipid” ND. HEPES buffer (750 μL) was added to separate 5 mg aliquots of CL and PC followed by vortexing to hydrate the lipids. Aliquots of these PC and CL dispersions were combined to achieve the indicated phospholipid weight ratios. ApoA-I was then added to the mixed lipid dispersions at a 5:2 (w/w) lipid:protein ratio. ND formation, as measured by sample clarification, was achieved by bath sonication at 48 °C for 2 min, alternating with bath sonication at 25 °C until sample absorbance was < 0.07 at 325 nm (< 10 min). For incubations with CaCl_2 , aliquots of mixed lipid ND, containing 78 nmol CL, were added to the wells of a microtiter plate. Indicated amounts of CaCl_2 in HEPES buffer were added to each well (final volume 200 μL) and the plate incubated for 1 h at 22 °C prior to sample absorbance measurements.

2.5. CL ND incubation with CaCl_2 and EDTA

CL ND were added to the wells of a microtiter plate as above. CaCl_2 (0 nmol, 600 nmol or 2000 nmol) was added and the samples incubated at 22 °C for 1 h. Following incubation, a 1:1 molar equivalent of EDTA to CaCl_2 was added to each sample. Total sample volumes after EDTA addition were maintained at 300 μL through addition of HEPES buffer. Samples were incubated for a further 1 h at 22 °C followed by absorbance measurement at 325 nm. In other experiments, EDTA-treated, CaCl_2 -modified CL ND were analyzed by gel filtration chromatography as described above before and after bath sonication at 48 °C for 3 min and centrifugation at 14,000 $\times g$ for 2 min.

2.6. Statistical analysis

Statistical analyses were performed by two-way ANOVA followed by Dunnett's test to compare treated samples against control samples (Figs. 2, 3, 4). Alternatively, the Holm-Sidak multiple *t*-test was used to compare the absorbance of CaCl_2 treated samples to CaCl_2 + EDTA treated samples (Fig. 5a). Statistical tests were performed using GraphPad Prism version 8.02 for Windows (GraphPad Software, San Diego, CA).

3. Results

3.1. Cardiolipin ND formulation and model structure

When aqueous dispersions of CL are incubated with apoA-I and subjected to bath sonication, lipid nanoparticle complex (i.e. ND) formation is evident by complete sample clarification [20]. Previous studies, using PC and other glycerophospholipids, revealed that ND exist as disk-shaped phospholipid bilayers whose perimeter is stabilized by interaction with apoA-I, an amphipathic α -helix-rich scaffold protein [21]. Unlike other glycerophospholipids that form ND, CL possesses a relatively small polar head group and four hydrophobic acyl chains, conferring a distinct cone-shaped structure to this lipid. Consistent with this, CL induces negative curvature pressure on bilayer membranes and is prone to adopting a non-bilayer state. With regard to the apparent ability of CL to form ND, it is conceivable that the apoA-I scaffold exerts

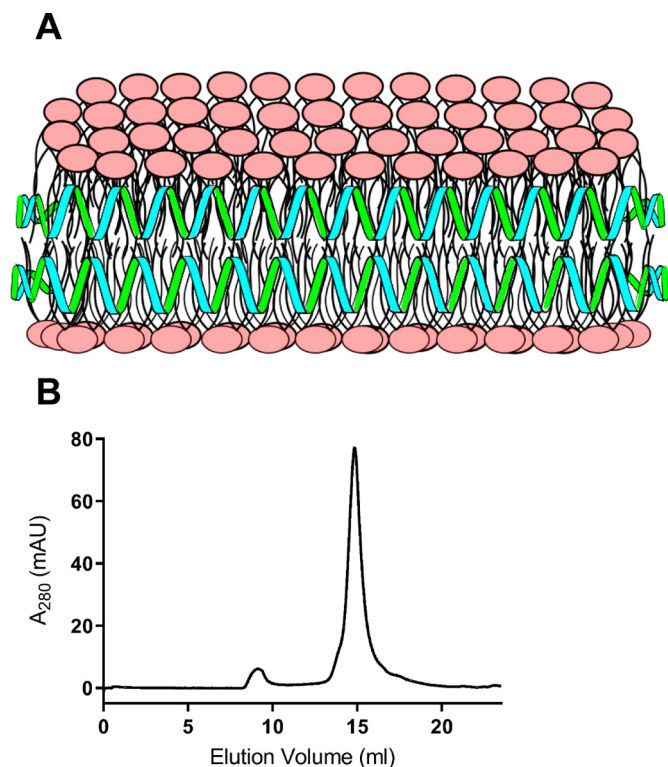


Fig. 1. Model structure of CL ND. A) In this depiction, CL (polar head groups in pink) is organized as a disk-shaped bilayer whose perimeter is circumscribed and stabilized by apoA-I (green/blue helices), which interacts with CL fatty acyl chains at the edge of the disk. B) FPLC size exclusion chromatography profile of CL ND. ND were formulated with apoA-I and CL as described. An aliquot of CL ND (0.32 mg apoA-I/0.8 mg CL) in 20 mM HEPES buffer, pH 7.2, was applied to a Superose 6 Increase 10/300 GL column and elution monitored at 280 nm.

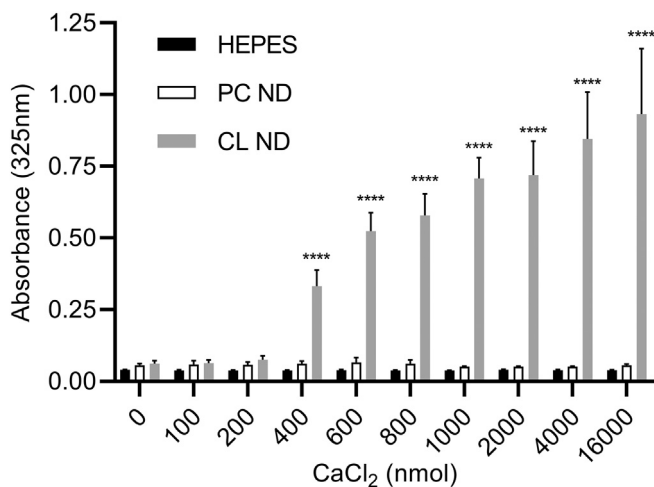


Fig. 2. Effect of CaCl₂ on ND sample integrity. ApoA-I containing PC ND and CL ND were formulated in HEPES buffer as described and aliquots of each (corresponding to 78 nmol CL or 147 nmol PC) were applied to the wells of a 96 well microtiter plate. To each well, indicated amounts of CaCl₂ (in HEPES buffer) were added and the volume adjusted to 200 μ L with HEPES buffer. The plate was incubated for 1 h at 22 $^{\circ}$ C and, following incubation, sample absorbance measured at 325 nm on a SpectraMax plate reader. Values reported are the mean \pm standard error (n = 9) ****, P < .0001 versus HEPES control and PC ND.

a belt-like stabilizing force around the ND bilayer perimeter, as depicted in Fig. 1A. In keeping with this model, FPLC gel filtration chromatography of CL ND (Fig. 1B) reveals a homogenous population

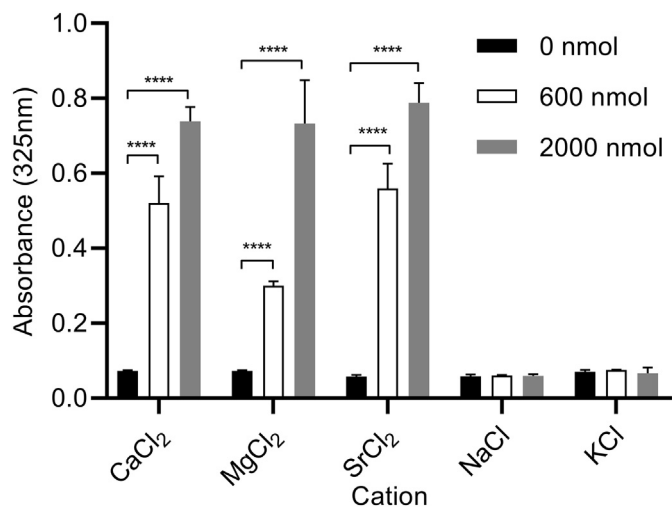


Fig. 3. Effect of alternate cations on ND sample integrity. Aliquots of CL ND (78 nmol CL), solubilized in HEPES buffer, were applied to the wells of a 96 well microtiter plate. To each well, specified quantities of the chloride salt of mono- or divalent cations was added and the volume adjusted to 200 μ L with HEPES buffer. The plate was incubated for 1 h at 22 $^{\circ}$ C followed by sample absorbance determination at 325 nm. Values reported are the mean \pm standard error (n = 3) ****, P < .0001 versus 0 nmol divalent cation.

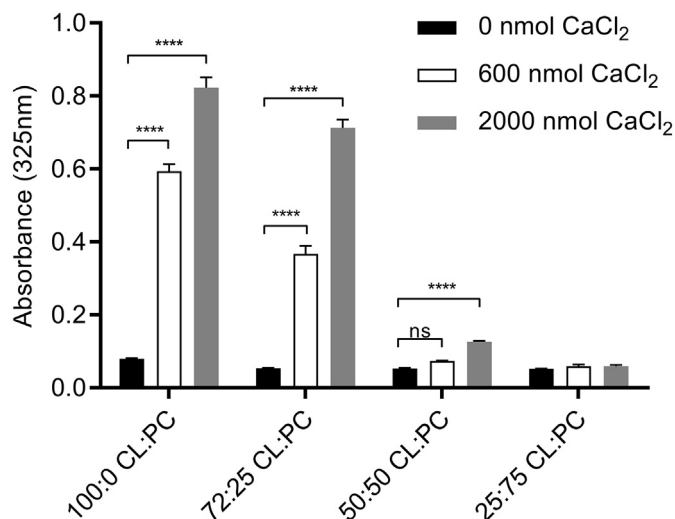


Fig. 4. Effect of calcium on mixed lipid ND sample integrity. ND containing specified weight ratios of CL and PC were formulated with apoA-I in HEPES buffer. Aliquots of the different ND samples (corresponding to 78 nmol CL), were added to the wells of a 96 well microtiter plate. To each well, indicated amounts of CaCl₂ were added and the volume adjusted to 200 μ L with HEPES buffer. The plate was incubated for 1 h at 22 $^{\circ}$ C and, following incubation, sample absorbance at 325 nm was measured. Values reported are the mean \pm standard error (n = 3) ****, P < .0001 versus 0 nmol CaCl₂. ns, not significant.

of particles in a similar size range to well characterized PC ND [25]. Thus, it may be considered that the scaffold function of apoA-I provides an opposing force to CL's tendency to transition to a non-bilayer state, thereby maintaining CL in a soluble bilayer state as ND.

3.2. The effect of CaCl₂ on ND sample turbidity

Both CL ND and PC ND are fully soluble in aqueous buffer. Negligible material precipitates upon centrifugation and samples remain stable for 1 week or more when stored at 4 $^{\circ}$ C. To determine the effect of CaCl₂ on ND structural integrity, PC ND and CL ND samples

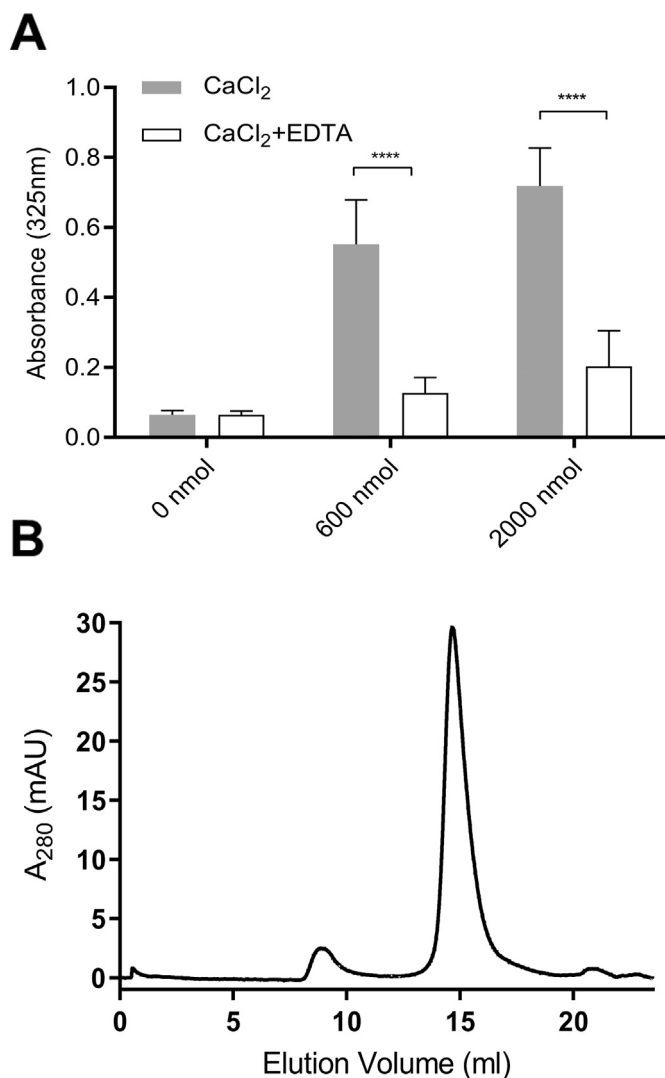


Fig. 5. Effect of EDTA on CaCl₂-disrupted CL ND. **A)** CL ND were formulated in HEPES buffer with apoA-I and aliquots corresponding to 78 nmol CL applied to the wells of a 96 well microtiter plate. Indicated amounts of CaCl₂ were added and the volume adjusted to 200 μ l with HEPES buffer. The plate was incubated for 1 h at 22 °C and, following incubation, sample absorbance at 325 nm was measured on a Spectramax plate reader. Subsequently, EDTA, dissolved in HEPES buffer, was added to each well to achieve a concentration equivalent to that of the added CaCl₂. The final volume of each well was adjusted to 300 μ l and the plate incubated for an additional 1 h at 22 °C. Following incubation, sample absorbance at 325 nm was measured. Values reported are the mean \pm standard error (n = 6) ****, P < .0001 calcium-treated versus EDTA-treated. **B)** FPLC size exclusion chromatography of EDTA-treated, CaCl₂-disrupted CL ND. A sample of CL ND (622 nmol CL), solubilized in HEPES buffer, was incubated with 8000 nmol CaCl₂ for 1 h at 22 °C to induce sample turbidity development. To this sample, 8000 nmol EDTA was added followed by incubation for 1 h at 22 °C to induce sample clarification. The clarified sample was bath sonicated at 48 °C for 2 min followed by chromatography on a Superose 6 Increase 10/300 GL FPLC column with elution monitored at 280 nm.

were incubated with increasing quantities of CaCl₂ for 1 h (Fig. 2). In control incubations containing HEPES buffer alone, CaCl₂ had no effect on sample absorbance at 325 nm. Likewise, when PC ND were incubated with CaCl₂, little or no change in sample absorbance occurred. By contrast, CL ND undergo a marked CaCl₂ concentration dependent increase in sample turbidity. The rate of this reaction was temperature dependent, with turbidity development occurring more rapidly at 37 °C than at 22 °C. Moreover, the physiologically relevant CL molecular species, tetralinoleoyl CL is capable for forming ND [20] and is also

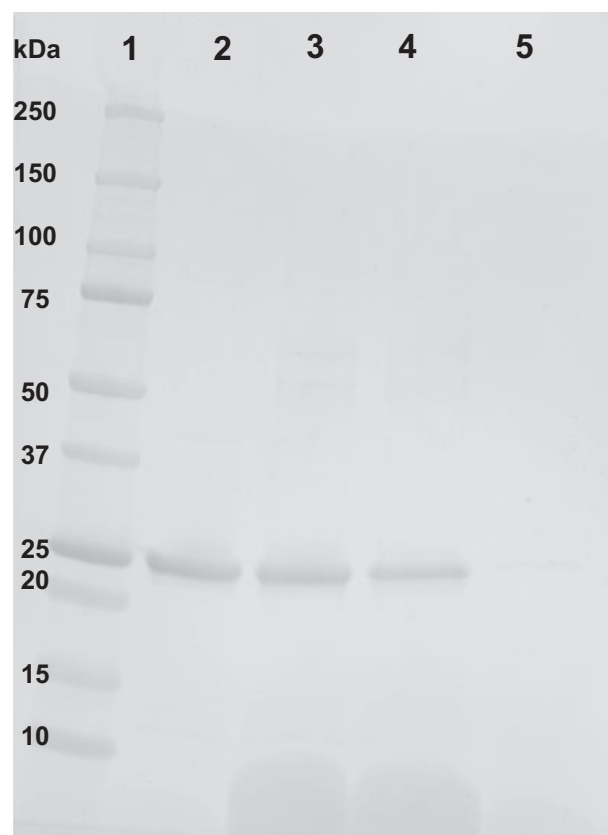


Fig. 6. Effect of CaCl₂-mediated disruption of CL ND on apoA-I solubility. CL ND were formulated with apoA-I in HEPES buffer and an aliquot, corresponding to 78 nmol CL, was incubated with 2000 nmol CaCl₂ for 1 h at 22 °C to induce sample turbidity development. Following this, the sample was centrifuged at 14,000 \times g for 2 min and the supernatant recovered. The precipitate was re-suspended in a volume of HEPES buffer equal to that of the reserved supernatant. Equivalent aliquots of the resuspended pellet and supernatant were electrophoresed on a 4–20% acrylamide gradient SDS PAGE gel and stained with GelCode Blue. Lane 1) molecular weight markers; Lane 2) apoA-I standard; Lane 3) control CL ND; Lane 4) CaCl₂-disrupted CL ND re-suspended pellet; Lane 5) CaCl₂-disrupted CL ND supernatant.

susceptible to CaCl₂ induced ND disruption (data not shown). As seen in Fig. 2, CaCl₂ levels below 400 nmol had little or no effect on CL ND sample turbidity. At 400 nmol CaCl₂, however, the sample became turbid and absorbance increased. As the amount of CaCl₂ was increased further, sample absorbance also increased, plateauing at 1000 nmol CaCl₂ / 78 nmol CL.

3.3. Effect of alternate cations on CL ND sample turbidity

To assess the cation specificity of the reaction induced by incubation with CaCl₂, CL ND (78 nmol CL) were incubated with increasing amounts of mono- or divalent cations (Fig. 3). CL ND in buffer alone served as control and, in the absence of added cations, remained fully soluble. Addition of CaCl₂ induced the expected concentration-dependent increase in CL ND sample absorbance and a similar trend was observed with MgCl₂ and SrCl₂. The monovalent cations, NaCl and KCl, had no effect on CL ND sample turbidity.

3.4. Effect of CaCl₂ on mixed phospholipid ND

To further explore CaCl₂ mediated effects on CL ND, different weight ratios of CL and PC were used to formulate ND. The resulting mixed phospholipid ND were incubated with CaCl₂. ND comprised of 100% CL, 75% CL, 50% CL and 25% CL were incubated in the absence

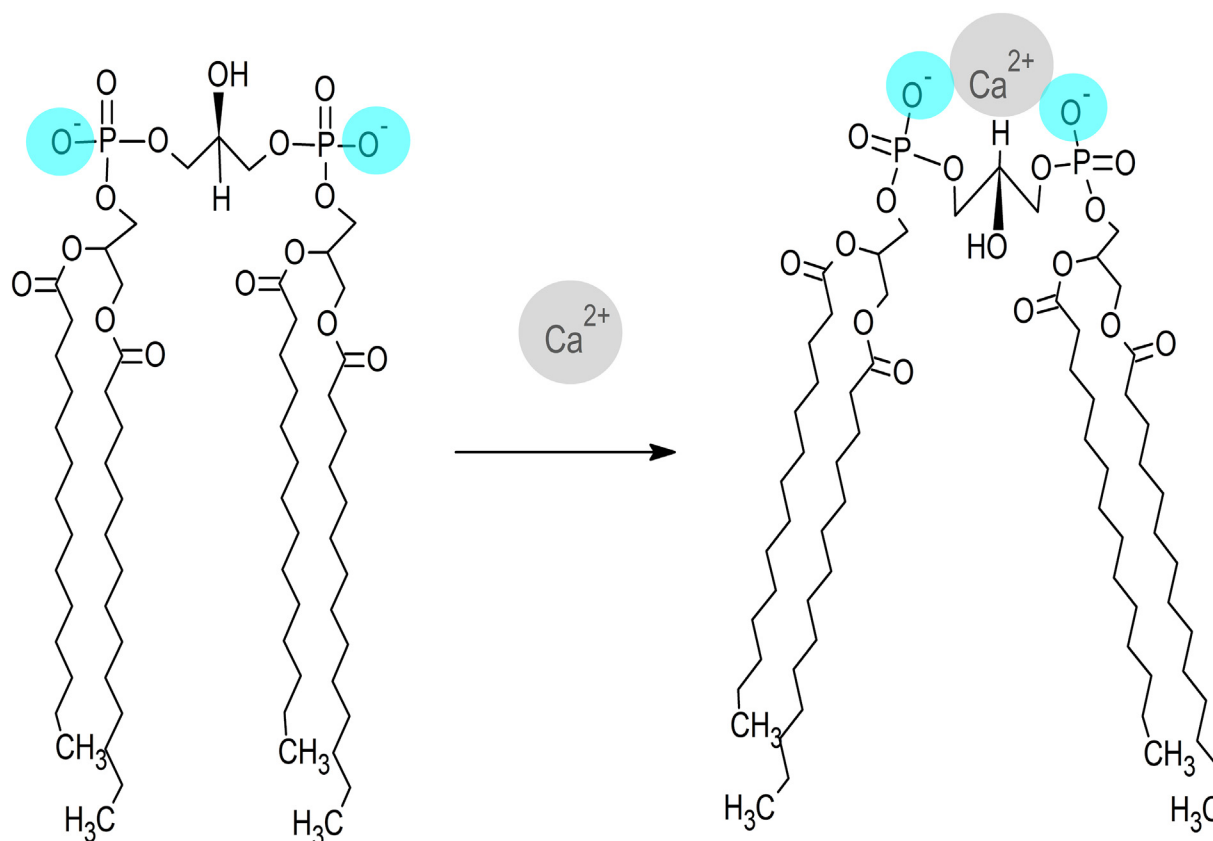


Fig. 7. Model depicting the effect of calcium binding on CL structure. Divalent cations, such as Ca^{2+} , are attracted to the anionic polar head group of CL, forming a bidentate binding interaction with its two phosphate moieties (blue). A single calcium ion localized between these phosphates induces structural repositioning of CL in order to maximize interaction with calcium. As the phosphate moieties converge toward the calcium ion, conformational strain is relieved by realignment of the CL fatty acyl chains, which results in the adoption of a conformation that is incompatible with a bilayer state.

or presence of 2 fixed amounts of CaCl_2 for 1 h, followed by measurement of sample turbidity (Fig. 4). The final CL content in each incubation was $100 \mu\text{g}$ (78 nmol). Similar to ND formulated with 100% CL, ND formulated at a 75:25 (w/w) ratio of CL to PC showed a strong CaCl_2 concentration-dependent increase in sample turbidity. ND formulated with a 50:50 (w/w) mixture of CL and PC showed a slight, but statistically significant, increase in absorbance at the highest CaCl_2 level tested. ND containing 25% CL and 75% PC were unaffected by incubation with CaCl_2 under these experimental conditions.

3.5. Effect of EDTA on CaCl_2 -induced CL ND sample turbidity

To determine whether chelation of added calcium by EDTA is able to reverse CaCl_2 -mediated effects on CL ND, samples of CL ND were incubated with CaCl_2 for 1 h to induce turbidity development. EDTA was then added (1:1 molar equivalence to CaCl_2) and the samples incubated for an additional 1 h, followed by absorbance determination at 325 nm (Fig. 5A). CL ND incubated with 600 nmol CaCl_2 , followed by 600 nmol EDTA, rapidly clarified. Samples treated with 2000 nmol CaCl_2 clarified more slowly upon addition of EDTA, returning to near original absorbance by the end of the 1 h incubation period. FPLC gel filtration analysis of CaCl_2 -treated CL ND samples clarified by incubation with EDTA revealed a slight increase in particle heterogeneity and centrifugation of this sample generated a small but reproducible precipitate (data not shown). However, bath sonication of EDTA clarified, CaCl_2 -treated CL ND did not give rise to a precipitate upon centrifugation and FPLC gel filtration chromatography (Fig. 5B) revealed a uniform population of particles whose elution characteristics were nearly indistinguishable from those of CL ND prior to incubation with CaCl_2 .

3.6. Effect of CaCl_2 on the interaction of apoA-I with CL

According to the model presented in Fig. 1, apoA-I is an essential structural component of CL ND. To determine whether apoA-I maintains contact with CL following incubation with CaCl_2 , insoluble material formed during this reaction was pelleted by centrifugation and the supernatant removed. Following re-suspension of pelleted material in a volume of buffer equal to the reserved supernatant, aliquots of each were subjected to SDS PAGE (Fig. 6). Densitometric scanning of the stained gel indicated > 90% of the apoA-I in the original CL ND sample was recovered in the insoluble fraction generated by incubation of CL ND with CaCl_2 . Analysis of the relative distribution of CL between the supernatant and pellet fractions using an assay based on binding of 10-N-nonyl acridine orange to CL indicated > 70% of the CL was recovered in the pellet with < 30% in the supernatant. Taken together, the data indicate that, following CaCl_2 -induced transition of CL to an insoluble, non-bilayer state, apoA-I remains associated with the lipid.

4. Discussion

CL is a uniquely structured glycerophospholipid that plays an important role in mitochondrial structure and bioenergetics. CL is a cone-shaped lipid, owing to a relatively small polar head group and four fatty acyl chains. Consistent with this molecular shape, CL exerts negative curvature pressure on membranes and is prone to adopt a non-bilayer, inverted hexagonal II phase. Despite this tendency, CL not only exists stably in mixed lipid membranes but can be induced to form an apparent nanoscale size planar bilayer when an aqueous dispersion of this lipid is bath sonicated in the presence of isolated recombinant human apoA-I. The complexes formed are fully soluble in neutral pH buffer,

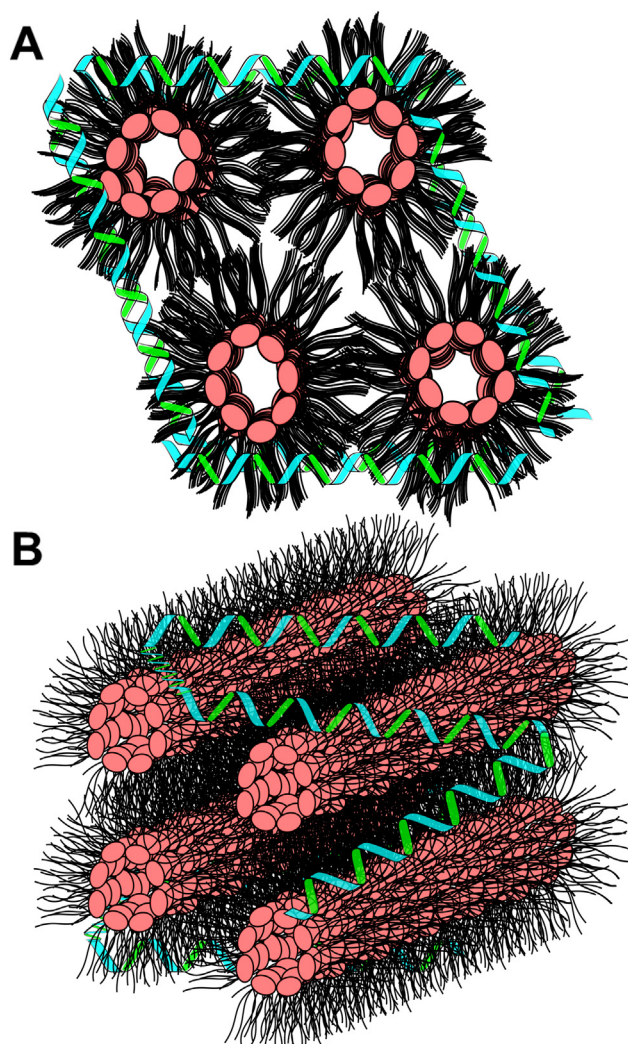


Fig. 8. Model of CaCl_2 -disrupted CL ND. After addition of CaCl_2 to CL ND, CL molecules transition to a non-bilayer state, presumably an inverted hexagonal II phase. In an inverted hexagonal II phase, the CL polar head groups (pink) align toward the center of lipid cylinders while CL fatty acyl chains (black) project into the aqueous milieu. Data presented indicates apoA-I (green/blue helices) remains associated with CL following CaCl_2 -mediated CL ND disruption. This association most likely involves apoA-I binding to exposed CL hydrocarbon tails, thereby providing some measure of protection from direct lipid interaction with the aqueous milieu. Upper image) End on depiction of CL in an inverted hexagonal II phase with apoA-I interacting with exposed acyl chains. Lower image) CL hexagonal II phase cylinders with associated apoA-I.

stable for extended periods when stored at 4 °C and, based on gel filtration chromatography, display a homogeneous particle size distribution. These complexes, comprised solely of CL and apoA-I, termed CL ND, represent a novel miniature membrane system to investigate CL's interactome.

One example of a CL binding partner is calcium. Upon incubation with CaCl_2 , fully soluble CL ND undergo a marked increase in sample turbidity, consistent with CL undergoing a transition from bilayer to non-bilayer state. This transition does not occur when PC ND are incubated with CaCl_2 . The reaction is CaCl_2 concentration dependent and changes in sample turbidity are detectable at a ~1:5 molar ratio of CL to CaCl_2 , while maximum sample absorbance values plateau at a ~1:12 molar ratio of CL to CaCl_2 . Mixed lipid ND that contain different ratios of CL and PC respond differently to CaCl_2 . The response is directly related to the CL content of the ND. Reducing the amount of CL in a given ND by replacing it with PC confers resistance against CaCl_2 -induced

transformation of ND from a soluble bilayer state to an insoluble non-bilayer state. Overall, these results reveal that decreasing the proportion of CL in ND decreases the absorbance increase induced by incubation with CaCl_2 . In other words, mixed lipid ND containing a lower proportion of CL per ND require more CaCl_2 to induce a bilayer to non-bilayer transition. This trend holds for ND formulated to possess 100%, 75%, 50% and 25% CL content.

The reaction described between CL ND and CaCl_2 also occurs when CL ND are incubated with other divalent cations, including MgCl_2 and SrCl_2 . Magnesium, which has the smallest atomic radius of the divalent cations tested, induced a lesser increase in sample absorbance than either calcium or strontium at the lower ion level tested. At higher amounts, however, all three divalent cations induced a similar increase in sample absorbance. On the other hand, incubation with monovalent cations across a wide concentration range had no discernable effect on CL ND. The specificity of this reaction for divalent cations suggests that the two negatively charged phosphate groups in CL's polar head group play a key role. Divalent cations, such as Ca^{2+} , are capable of forming a bidentate binding interaction with these phosphates, as depicted in Fig. 7. Moreover, it is anticipated that, as the two phosphates reposition to increase contact with the Ca^{2+} ion, conformational strain is placed on other parts of the CL molecule. This strain may be relieved by repositioning the hydrocarbon tails of CL in a manner that further accentuates its cone shape. Such a change in the orientation of CL hydrocarbon tails, relative to the polar head group, is postulated to accentuate the conical shape of CL, decreasing its ability to stably reside in planar bilayer structure of ND. It is likely such a molecular shape change, induced by calcium binding, ultimately leads to disruption of the ND bilayer structure and the transition of CL from a soluble bilayer to an insoluble non-bilayer state that ultimately precipitates from solution. This calcium-induced bilayer disruption may relate to other biological interactions in the CL interactome. In particular, release of cytochrome c from the inner mitochondrial membrane may be related to an influx of calcium into the mitochondria, though the exact mechanism remains under investigation [26,27]. In any event, CL ND may be a viable model for examining this interaction in a controlled, readily accessible *in vitro* setting.

Whereas it is considered that the apolipoprotein scaffold surrounding the disk-shaped bilayer of ND exerts a stabilizing force that “holds” CL in a bilayer phase through direct contact of its amphipathic α -helices with otherwise exposed fatty acyl chains around the edge of the discoidal bilayer (see Fig. 1), the data indicate calcium-mediated effects on CL structure exert an opposing force that, above a certain threshold, results in CL ND particle disruption. Based on experiments conducted with mixed phospholipid ND, as the CL content of a given ND formulation is increased, the easier it is for the stabilizing influence of the apolipoprotein to be exceeded by incubation with CaCl_2 .

Once the scaffold protein's stabilizing force is exceeded, CL undergoes a bilayer to non-bilayer transition and this process coincides with obvious changes in sample turbidity. Remarkably, however, upon addition of EDTA, which effectively chelates all calcium present, including that bound to CL, an environment is created wherein apoA-I is capable of re-solubilizing CL, presumably by reconstitution of CL ND. FPLC analysis revealed that bath sonication of EDTA clarified, CaCl_2 -treated CL ND gives rise to an elution profile that is nearly indistinguishable from that of the starting CL ND. The observation that the reaction induced by CaCl_2 can be reversed by the addition of EDTA may be related to the fact that, following CaCl_2 mediated disruption of CL ND, apoA-I remains associated with the insoluble CL precipitate. Assuming Ca^{2+} bound CL adopts a hexagonal II phase, then it is likely that apoA-I maintains a binding interaction with exposed hydrocarbon tails at the aqueous interface of this insoluble lipid phase, thereby minimizing contact between hydrophobic CL fatty acyl chains and the aqueous milieu, as depicted in Fig. 8. Maintenance of a binding interaction between apoA-I and CL in the CaCl_2 disrupted state is likely a key factor in the ability of EDTA to promote re-formation of intact CL ND.

Just as the initial formation of CL ND required bath sonication to generate a uniform homogenous population of CL ND, following EDTA treatment of CaCl₂ disrupted CL ND, bath sonication yielded a single major population of CL ND.

It is noteworthy that the major CL molecular species found in mitochondria of heart and muscle tissue is tetralinoleoyl CL. This molecular species is generated by acyl chain remodeling of nascent CL through the action of a transacylase termed tafazzin [28]. Although the potential benefits of establishing a uniform fatty acyl distribution in CL are not known, it has been shown that tafazzin activity in vitro is optimal when CL exists in a non-bilayer state [29]. Insofar as tetralinoleoyl CL is capable of forming ND and is susceptible to CaCl₂ mediated conversion to a non-bilayer state, this system may provide a model for understanding the role(s) of calcium in CL remodeling and its role in maintenance of mitochondrial membrane integrity.

Transparency document

The [Transparency document](#) associated with this article can be found, in online version.

Acknowledgements

This work was supported by a grant from the National Institutes of Health (R37 HL64159). The authors thank Sharon Young, Irina Romenskaia, Jennifer Shearer and Mohamad Dandan for contributing to the development of this research.

References

- [1] S.E. Horvath, G. Daum, Lipids of mitochondria, *Prog. Lipid Res.* 52 (2013) 590–614.
- [2] P.R. Cullis, B. de Kruijff, Lipid polymorphism and the functional roles of lipids in biological membranes, *Biochim. Biophys. Acta* 559 (1979) 399–420.
- [3] N. Stepanyants, P.J. Macdonald, C.A. Francy, J.A. Mears, X. Qi, R. Ramachandran, Cardiolipin's propensity for phase transition and its reorganization by dynamine-related protein 1 form a basis for mitochondrial membrane fission, *Mol. Biol. Cell* 26 (2015) 3104–3116.
- [4] L.D. Renner, D.B. Weibel, Cardiolipin microdomains localize to negatively curved regions of *E. coli* membranes, *Proc. Natl. Acad. Sci. U. S. A.* 108 (2011) 6264–6269.
- [5] R. Lewis, R.N. McElhaney, The physicochemical properties of cardiolipin bilayers and cardiolipin-containing lipid membranes, *Biochim. Biophys. Acta* 1788 (2009) 2069–2079.
- [6] N. Ikon, R.O. Ryan, Cardiolipin and mitochondrial cristae organization, *Biochim. Biophys. Acta* 1859 (2017) 1156–1163.
- [7] P.S. Brookes, Y. Yoon, J.L. Robotham, M.W. Anders, S.S. Sheu, Calcium, ATP, and ROS: a mitochondrial love-hate triangle, *Am J Physiol Cell Physiol.* 287 (2004) C817–C833.
- [8] G. Paradies, G. Petrosillo, V. Paradies, F.M. Ruggiero, Role of cardiolipin peroxidation and Ca²⁺ in mitochondrial dysfunction and disease, *Cell Calcium* 45 (2009) 643–650.
- [9] F. Celsi, P. Pizzo, M. Brini, S. Leo, C. Fotino, P. Pinton, R. Rizzuto, Mitochondria, calcium, and cell death: a deadly triad in neurodegeneration, *Biochim. Biophys. Acta Bioenerg.* 1787 (5) (2009) 335–344.
- [10] T. Peng, M.J. Jou, Oxidative stress caused by mitochondrial calcium overload, *Ann. N. Y. Acad. Sci.* 1201 (2010) 183–188.
- [11] R.P. Rand, S. Sengupta, Cardiolipin forms hexagonal structures with divalent cations, *Biochim. Biophys. Acta* 255 (1972) 484–492.
- [12] B. De Kruijff, A.J. Verkleij, J. Leunissen-Bijvelt, C.J.A. Van Echteld, J. Hille, H. Rijnbout, Further aspects of the calcium dependent polymorphism of bovine heart cardiolipin, *Biochim. Biophys. Acta* 693 (1982) 1–12.
- [13] G.L. Kirk, S.M. Gruner, D.L. Stein, A thermodynamic model of the lamellar to inverse hexagonal phase transition of lipid membrane-water systems, *Biochemistry* 23 (1984) 1093–1102.
- [14] P.R. Cullis, A.J. Verkleij, P.H.J. Ververgaert, Polymorphic phase behaviour of cardiolipin as detected by ³¹P NMR and freeze-fracture techniques. Effects of calcium, dibucaine and chlorpromazine, *Biochim. Biophys. Acta* 513 (1978) 11–20.
- [15] E.B. Smaal, C. Schreuder, J.B. van Baal, P.N.M. Tjiburg, J.G. Mandersloot, B.D. Kruijff, J.D. Gier, Calcium-induced changes in permeability of dioleoylphosphatidylcholine model membranes containing bovine heart cardiolipin, *Biochim. Biophys. Acta* 897 (1987) 191–196.
- [16] P.M. Macdonald, J. Seelig, Calcium binding to mixed cardiolipin-phosphatidylcholine bilayers as studied by deuterium nuclear magnetic resonance, *Biochemistry.* 26 (1987) 6292–6298.
- [17] A. Sharma, U.S. Sharma, Liposomes in drug delivery: progress and limitations, *Int. J. Pharm.* 154 (1997) 123–140.
- [18] A. Akbarzadeh, R. Rezaei-Sadabady, S. Davaran, S.W. Joo, N. Zarghami, Y. Hanifehpour, M. Samiei, M. Kouhi, K. Nejati-Koshki, Liposome: classification, preparation, and applications, *Nanoscale Res. Lett.* 8 (2013) 102.
- [19] F. Bozzuto, A. Molinari, Liposomes as nanomedical devices, *Int. J. Nanomedicine* 10 (2015) 975–999.
- [20] N. Ikon, B. Su, F. Hsu, T.M. Forte, R.O. Ryan, Exogenous cardiolipin localizes to mitochondria and prevents TAZ knockdown-induced apoptosis in myeloid progenitor cells, *Biochem Biophys Res Comm* 464 (2015) 580–585.
- [21] R.O. Ryan, Nanobiotechnology applications of reconstituted high density lipoprotein, *J. Nanobiotech.* 8 (2010) 8–28.
- [22] R.O. Ryan, T.M. Forte, M.N. Oda, Optimized bacterial expression of human apolipoprotein A-I, *Protein Expr. Purif.* 27 (2003) 98–103.
- [23] C.T. Rueden, J. Schindelin, M.C. Hiner, B.E. DeZonia, A.E. Walter, E.T. Arena, K.W. Eliceiri, ImageJ2: ImageJ for the next generation of scientific image data, *BMC Bioinformatics* 18 (2017) 529.
- [24] M.I. Garcia Fernandez, D. Ceccarelli, U. Muscatello, Use of the fluorescent dye 10-N-nonyl acridine orange in quantitative and location assays of cardiolipin: a study of different experimental models, *Anal. Biochem.* 328 (2004) 174–180.
- [25] M. Wadsater, S. Maric, J.B. Simonsen, K. Mortensen, M. Cardenas, The effect of using binary mixtures of zwitterionic and charged lipids on nanodisc formation and stability, *Soft Matter* 9 (2013) 2329–2337.
- [26] J. Prudent, H.M. McBride, The mitochondria-endoplasmic reticulum contact sites: a signaling platform for cell death, *Curr. Opin. Cell Biol.* 47 (2017) 52–63.
- [27] C. Giorgi, F. Baldassari, A. Bononi, M. Bonora, E.D. Marchi, S. Marchi, S. Missiroli, S. Patergnani, A. Rimessi, J.M. Suski, M.R. Wieckowski, P. Pinton, Mitochondrial Ca²⁺ and apoptosis, *Cell Calcium* 52 (2012) 36–43.
- [28] M. Schlame, Cardiolipin remodeling and the function of tafazzin, *Biochim. Biophys. Acta* 1831 (2013) 582–588.
- [29] M. Schlame, D. Acehan, B. Berno, Y. Xu, S. Valvo, M. Ren, D.L. Stokes, R.M. Epanand, The physical state of lipid substrates provides transacylation specificity for tafazzin, *Nat. Chem. Biol.* 8 (2012) 862–869.